

# Efficient Large-Scale Language Model Training on GPU Clusters

Deepak Narayanan<sup>†‡</sup>, Mohammad Shoeybi<sup>†</sup>, Jared Casper<sup>†</sup>, Patrick LeGresley<sup>†</sup>,  
Mostofa Patwary<sup>†</sup>, Vijay Korthikanti<sup>†</sup>, Dmitri Vainbrand<sup>†</sup>, Prethvi Kashinkunti<sup>†</sup>,  
Julie Bernauer<sup>†</sup>, Bryan Catanzaro<sup>†</sup>, Amar Phanishayee<sup>\*</sup>, Matei Zaharia<sup>‡</sup>  
<sup>†</sup>NVIDIA <sup>‡</sup>Stanford University <sup>\*</sup>Microsoft Research

## ABSTRACT

Large language models have led to state-of-the-art accuracies across a range of tasks. However, training these large models efficiently is challenging for two reasons: a) GPU memory capacity is limited, making it impossible to fit large models on a single GPU or even on a multi-GPU server; and b) the number of compute operations required to train these models can result in unrealistically long training times. New methods of model parallelism such as tensor and pipeline parallelism have been proposed to address these challenges; unfortunately, naive usage leads to fundamental scaling issues at thousands of GPUs due to various reasons, e.g., expensive cross-node communication or idle periods waiting on other devices.

In this work, we show how to compose different types of parallelism methods (tensor, pipeline, and data parallelism) to scale to thousands of GPUs, achieving a two-order-of-magnitude increase in the sizes of models we can efficiently train compared to existing systems. We discuss various implementations of pipeline parallelism and propose a novel schedule that can improve throughput by more than 10% with comparable memory footprint compared to previously-proposed approaches. We quantitatively study the trade-offs between tensor, pipeline, and data parallelism, and provide intuition as to how to configure distributed training of a large model. The composition of these techniques allows us to perform training iterations on a model with 1 trillion parameters at 502 petaFLOP/s on 3072 GPUs with achieved per-GPU throughput of 52% of peak; previous efforts to train similar-sized models achieve much lower throughput (36% of theoretical peak). Our code has been open-sourced at <https://github.com/nvidia/megatron-lm>.

## 1 INTRODUCTION

Transformer-based language models [10, 21, 25–27, 33, 36] in Natural Language Processing (NLP) have driven rapid progress in recent years as computation at scale has become more available and datasets have become larger. At the same time, recent work [8, 31] has shown large language models to be effective zero- or few-shot learners, with high accuracy on many NLP tasks and datasets. As a result, the number of parameters in state-of-the-art NLP models have grown at an exponential rate (Figure 1). Training such models, however, is challenging for two reasons: (a) it is no longer possible to fit the parameters of these models in the main memory of even the largest GPU (NVIDIA recently released 80GB-A100 cards), (b) even if we are able to fit the model in a single GPU (e.g., by swapping parameters between host and device memory), the high number of compute operations required can result in unrealistically long training times without model parallelism (e.g., training GPT-3 with 175 billion parameters [8] would require approximately 36 years with 8 V100 GPUs or 7 months with 512 V100 GPUs assuming perfect data-parallel scaling, both unreasonable training times).

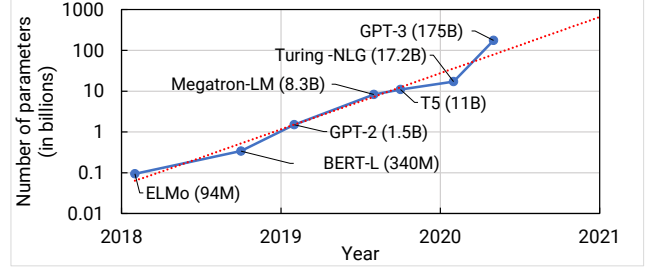


Figure 1: Trend of sizes of state-of-the-art Natural Language Processing (NLP) models with time. The number of floating-point operations to train these models is increasing proportionally.

Various model parallelism techniques have been proposed to address these two challenges. For example, recent work [30, 31] has shown how tensor (intra-layer) model parallelism, where matrix multiplications within each transformer layer are split over multiple GPUs, can be used to overcome these limitations. Although this approach works well for models of sizes up to 20 billion parameters on NVIDIA DGX A100 servers (with 8 80GB-A100 GPUs), it breaks down for larger models. Larger models need to be split across multiple multi-GPU servers, which leads to two problems: (a) the all-reduce communication required for tensor parallelism needs to go through inter-server links, which are slower than the high-bandwidth NVLink links available within a multi-GPU server, (b) a high degree of model parallelism can create small GEMMs, potentially decreasing GPU utilization.

Pipeline model parallelism [11, 15, 18, 22, 23, 35] is another technique to support the training of large models, where layers of a model are striped over multiple GPUs. A batch is split into smaller microbatches, and execution is pipelined across these microbatches. Layers can be assigned to workers in various ways, and various schedules for the forward and backward passes of inputs can be used. Each of these layer assignment and scheduling strategies leads to different performance tradeoffs. Regardless of schedule, to preserve strict optimizer semantics, optimizer steps need to be synchronized across devices, leading to a *pipeline flush* at the end of every batch where microbatches in a batch are allowed to complete execution (and no new microbatches are injected). As much as 50% of time can be spent flushing the pipeline depending on the number of microbatches injected into the pipeline. The larger the ratio of number of microbatches to the pipeline size, the smaller the time spent in the pipeline flush. Therefore, to achieve high efficiency, a large batch size is often necessary.

Users can thus train their large models using various techniques, each with different tradeoffs. Moreover, these techniques can be *combined*; however, combining these techniques leads to non-trivial

interactions, which need to be reasoned through carefully for good performance. In this paper, we try to answer the following question:

*How should parallelism techniques be combined to maximize the training throughput of large models given a batch size while retaining strict optimizer semantics?*

In particular, we show how to combine tensor, pipeline, and data parallelism to train large language models with extremely good performance. The combination of tensor parallelism within a multi-GPU server, pipeline parallelism across multi-GPU servers, and data parallelism, allows us to practically train models with a trillion parameters with graceful scaling in a highly-optimized cluster environment with high-bandwidth links between GPUs on the same server and across servers. We can use similar ideas to train larger models as well, given more training resources. In our experiments, we demonstrate close to linear scaling to 3072 A100 GPUs, with an achieved end-to-end training throughput of 163 teraFLOP/s per GPU (including communication, data preprocessing, and optimization), which is 52% of peak device throughput (312 teraFLOP/s), and an aggregate throughput of 502 petaFLOP/s, on a GPT model [8] with a trillion parameters and 16-bit precision. We believe this is the fastest training throughput achieved for this size of model: past systems [22, 31] cannot train such large models, and DeepSpeed [1], which also combines data, tensor, and pipeline parallelism, achieves much lower throughput (37.6 petaFLOP/s, 36% of theoretical peak) using 800 V100 GPUs.

Achieving this throughput at scale required innovation and careful engineering along multiple axes: efficient kernel implementations that allowed most of the computation to be compute-bound as opposed to memory-bound, smart partitioning of computation graphs over the devices to reduce the number of bytes that need to be sent over network links while also limiting device idle periods, domain-specific communication optimization, and fast hardware (state-of-the-art GPUs and high-bandwidth links between GPUs on the same and different servers). Our software implementation is open sourced at <https://github.com/nvidia/megatron-lm>; we are hopeful that this will enable other groups to train large NLP models efficiently at scale.

In addition, we studied the interaction between the various components affecting throughput, both empirically and analytically. Based on these studies, we offer the following guiding principles on how to configure distributed training:

- The parallelization strategy has an impact on the amount of communication, the compute efficiency with which kernels are executed, as well as the idle time workers spend waiting for computation due to pipeline flushes (pipeline bubbles). For example, in our experiments, we found that sub-optimal combinations of tensor and pipeline model parallelism can lead to up to  $2\times$  lower throughput, even with high-bandwidth network links between servers; tensor model parallelism is effective within a multi-GPU server, but pipeline model parallelism must be used for larger models.
- The schedule used for pipeline parallelism has an impact on the amount of communication, the pipeline bubble size, and memory used to store activations. We propose a novel interleaved schedule that can improve throughput by as

much as 10% compared to previously-proposed schedules [15, 23] with comparable memory footprint.

- Values of hyperparameters such as microbatch size have an impact on the memory footprint and the arithmetic efficiency of kernels executed on the worker. In our experiments, the optimal value of the microbatch size is problem-dependent and can increase training throughput by up to 15%.
- At scale, distributed training is communication-intensive. When training a trillion-parameter model on 3072 GPUs, our implementation used an effective bisection bandwidth of 892 GB/s for pipeline-parallel communication, and 13 TB/s for data-parallel communication. Using slower interconnects across nodes or more communication-intensive partitionings across devices would hinder scaling performance.

We do not automatically explore the search space of parallelism strategies (such as FlexFlow [17]), but instead suggest heuristics (in §3) that we found work well in practice. We leave auto-optimization to future work.

## 2 MODES OF PARALLELISM

In this section, we discuss the parallelism techniques that facilitate the *efficient* training of large models that do not fit in the memory of a single GPU. In this work, we combine tensor model parallelism and pipeline model parallelism (shown in Figure 2), with data parallelism.

### 2.1 Data Parallelism

With data parallelism [19, 34], each worker has a copy of the full model, the input dataset is sharded, and workers aggregate their gradients periodically to ensure that all workers see a consistent version of the weights. For large models which do not fit on a single worker, data parallelism can be used on smaller model shards.

### 2.2 Pipeline Model Parallelism

With pipeline parallelism, the layers of a model are sharded across multiple devices. When used on repetitive transformer-based models, each device can be assigned an equal number of transformer layers. We do not consider more asymmetric model architectures, where assignment of layers to pipeline stages is harder; we defer to related work [17, 22, 32] to solve this problem.

A batch is split into smaller microbatches; execution is then pipelined across microbatches. Pipelining schemes need to ensure that inputs see consistent weight versions across forward and backward passes for a particular input for well-defined weight update semantics. Specifically, naive pipelining can lead to an input seeing weight updates in the backward pass not seen in the forward pass.

To retain strict optimizer semantics *exactly*, we introduce periodic pipeline flushes so that optimizer steps are synchronized across devices. At the start and end of every batch, devices are idle. We call this idle time the *pipeline bubble*, and want to make it as small as possible. Asynchronous and bounded-stale approaches such as PipeMare, PipeDream, and PipeDream-2BW [18, 22, 23, 35] do away with flushes completely, but relax weight update semantics. We defer consideration of such schemes to future work.

There are several possible ways of scheduling forward and backward microbatches across devices; each approach offers different

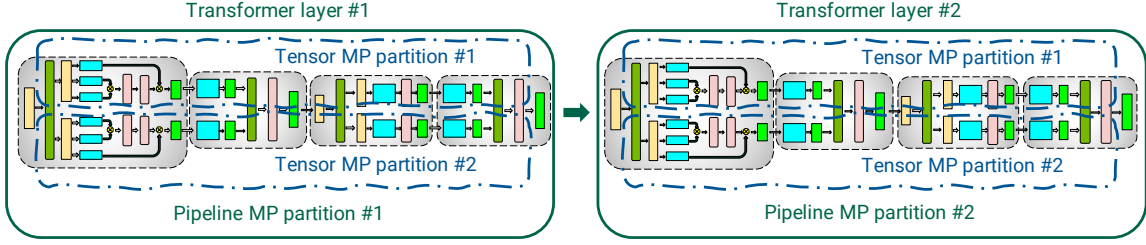


Figure 2: Combination of tensor and pipeline model parallelism (MP) used in this work for transformer-based models.

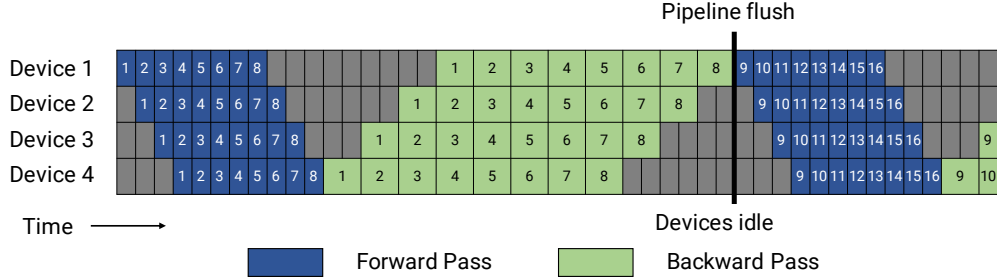


Figure 3: Pipeline schedule with forward passes (blue) for all microbatches (represented by numbers) followed by backward passes (green). The gray area represents the pipeline bubble time. For simplicity, we assume that the backward pass takes twice as long as forward pass. The efficiency of the pipeline schedule does not depend on this factor. Each batch in this example consists of 8 microbatches, and the number is a unique identifier given to the corresponding microbatch. The optimizer is stepped and weight parameters updated at the pipeline flush to ensure strict optimizer semantics, leading to idle devices and a pipeline bubble.

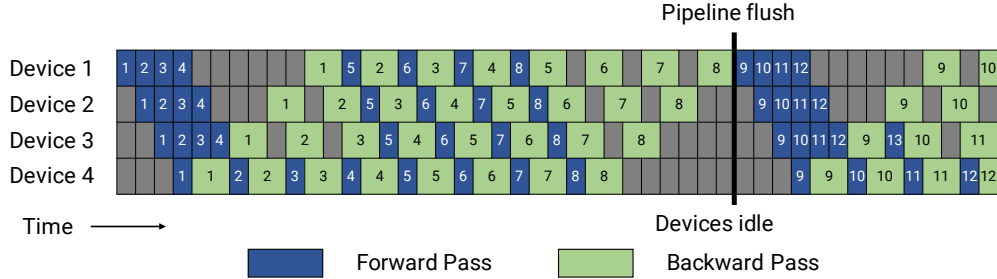


Figure 4: Pipeline schedule with 1F1B schedule (initial warm-up followed by alternating forward and backward passes in steady state).

tradeoffs between pipeline bubble size, communication, and memory footprint. We discuss two such approaches in this section.

**2.2.1 Default Schedule.** GPipe [15] proposes a schedule where the forward passes for all microbatches in a batch are first executed, followed by backward passes for all microbatches (shown in Figure 3). The size of GPipe’s pipeline bubble ( $t_{pb}$ ) can easily be quantified. We denote the number of microbatches in a batch as  $m$ , the number of pipeline stages (equal to number of devices used for pipeline parallelism here) as  $p$ , the ideal time per iteration as  $t_{id}$  (assuming perfect / ideal scaling), and the time to execute a single microbatch’s forward and backward pass as  $t_f$  and  $t_b$ . For the schedule in Figure 3, the pipeline bubble consists of  $p - 1$  forward passes at the start of a batch, and  $p - 1$  backward passes at the end. The total amount of time spent in the pipeline bubble is then

$t_{pb} = (p - 1) \cdot (t_f + t_b)$ . The ideal processing time spent in the batch is  $t_{id} = m \cdot (t_f + t_b)$ . Therefore, the fraction of ideal computation time spent in the pipeline bubble is:

$$\text{Bubble time fraction} = \frac{t_{pb}}{t_{id}} = \frac{p - 1}{m}.$$

For the bubble time fraction to be small, we thus need  $m \gg p$ . For such large  $m$ , this approach has a high memory footprint as it requires stashed intermediate activations (or just input activations for each pipeline stage when using activation recomputation) to be kept in memory for all  $m$  microbatches through the lifetime of a training iteration.

Instead, we use the PipeDream-Flush schedule [23]. In this schedule, we first enter a warm-up phase where workers perform differing numbers of forward passes as shown in Figure 4. This schedule

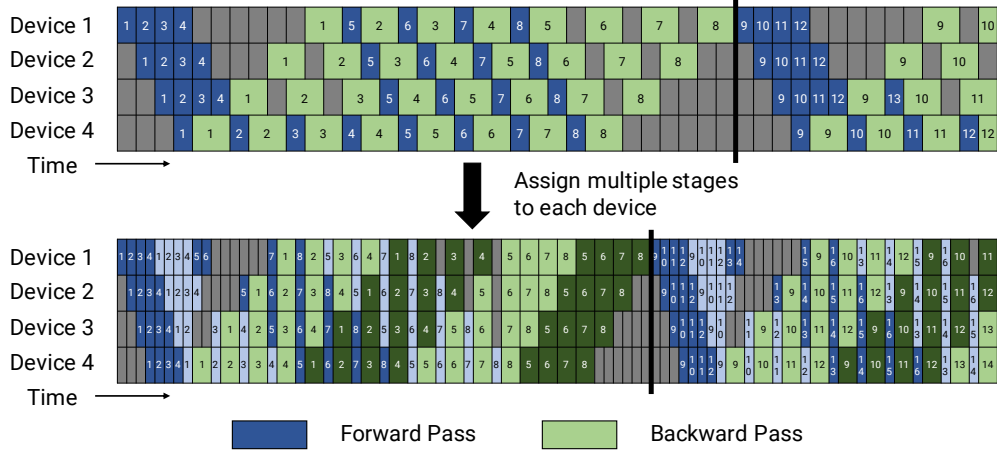


**Figure 5: New interleaved 1F1B schedule, where each device is assigned multiple stages (in this case, 2). Dark colors show the first stage and light colors show the second stage. Additional communication is required since the number of stages is doubled, but the size of the pipeline bubble is decreased (the pipeline flush happens sooner in the interleaved timeline).**

limits the number of in-flight microbatches (the number of microbatches for which the backward pass is outstanding and activations need to be maintained) to the depth of the pipeline, instead of the number of microbatches in a batch. After the warm-up phase, each worker then enters a steady state, where workers perform one forward pass followed by one backward pass (1F1B for short). Finally, at the end of a batch, we complete backward passes for all remaining in-flight microbatches. The time spent in the bubble is the same for this new schedule, but the number of outstanding forward passes is at most the number of pipeline stages for the schedule in Figure 4. As a result, this schedule requires activations to be stashed for  $p$  or fewer microbatches (compared to  $m$  microbatches for the schedule in Figure 3). When  $m \gg p$ , the schedule in Figure 4 is consequently much more memory-efficient than the one in Figure 3.

**2.2.2 Schedule with Interleaved Stages.** To reduce the size of the pipeline bubble, each device can perform computation for multiple subsets of layers (called a model chunk), instead of a single contiguous set of layers. For example, if each device had 4 layers before (i.e., device 1 had layers 1 – 4, device 2 had layers 5 – 8, and so on), we could have each device perform computation for two model chunks (each with 2 layers), i.e., device 1 has layers 1, 2, 9, 10; device 2 has layers 3, 4, 11, 12; and so on. With this scheme, each device in the pipeline is assigned multiple stages.

As before, we can use an “all-forward, all-backward” version of this schedule, but this has a high memory footprint (proportional to  $m$ ). Instead, we developed an interleaved schedule to use the more memory-efficient 1F1B schedule from before. This new schedule is shown in Figure 5, and requires the number of microbatches in a batch to be an integer multiple of the degree of pipeline parallelism (number of devices in the pipeline). For example, with 4 devices, the number of microbatches in a batch must be a multiple of 4.

As shown in Figure 5, the pipeline flush for the same batch size happens sooner in the new schedule. If each device has  $v$  stages (or model chunks), then the forward and backward time for a microbatch for each stage will now be  $t_f/v$  and  $t_b/v$ , respectively.

Thus the pipeline bubble time reduces to  $t_{pb}^{\text{int.}} = \frac{(p-1) \cdot (t_f + t_b)}{v}$ , and the bubble time fraction is then:

$$\text{Bubble time fraction} = \frac{t_{pb}^{\text{int.}}}{t_{id}} = \frac{1}{v} \cdot \frac{p-1}{m}.$$

This means that the new schedule reduces the bubble time by  $v$ . This reduced pipeline bubble size, however, does not come for free: this schedule requires extra communication. Quantitatively, the amount of communication also increases by  $v$  (the total number of stages increases by  $v$ ). In the next section, we discuss how we can utilize the 8 InfiniBand networking cards in a multi-GPU server (e.g., DGX A100 node) to reduce the impact of this extra communication.

## 2.3 Tensor Model Parallelism

With tensor model parallelism, individual layers of the model are partitioned over multiple devices. In this paper, we use the particular partitioning strategy used by Megatron [31] for transformer layers that are the bedrock of language models. We can apply similar ideas to other types of models, like CNNs, as well. We briefly outline this strategy below.

A transformer layer consists of a self-attention block followed by a two-layer multi-layer perceptron (MLP). Further details of the transformer layer can be found in Vaswani et al [33].

The MLP block consists of two GEMMs with a GeLU non-linearity in the middle:

$$Y = \text{GeLU}(XA) \quad Z = \text{Dropout}(YB)$$

We can split  $A$  along its columns  $A = [A_1, A_2]$ . This partitioning allows the GeLU non-linearity to be independently applied to the output of each partitioned GEMM:

$$[Y_1, Y_2] = [\text{GeLU}(XA_1), \text{GeLU}(XA_2)]$$

This is advantageous as it removes the need for synchronization (needed if  $A$  is split along its rows since GeLU is non-linear).

The rows of the second weight matrix  $B$  can then be split along its rows to remove the need for any communication between the

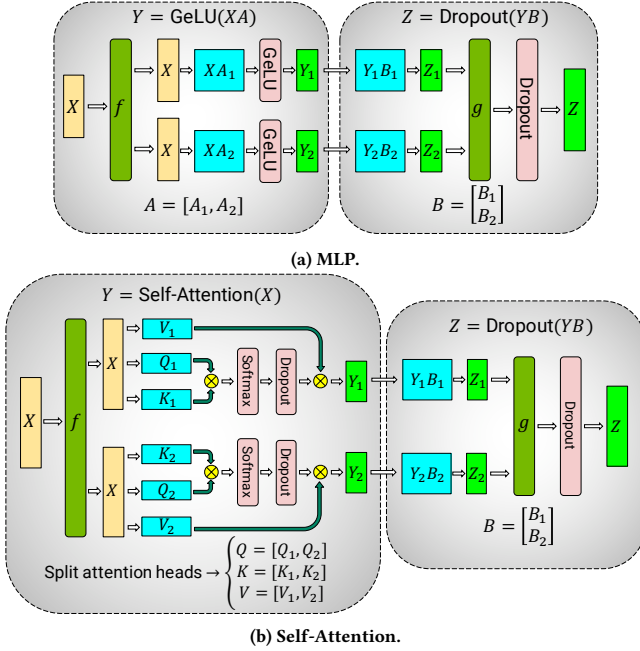


**Figure 6: Blocks of Transformer with Tensor Model Parallelism (borrowed from Megatron [31]).**  $f$  and  $g$  are conjugate.  $f$  is the identity operator in the forward pass and all-reduce in the backward pass, while  $g$  is the reverse.

GEMMs (shown in Figure 6a), as shown below:

$$B = \begin{bmatrix} B_1 \\ B_2 \end{bmatrix}, Y = [Y_1, Y_2].$$

The output of the second GEMM is then reduced across the GPUs before the dropout layer.

We exploit the inherent parallelism in the multi-head attention operation to partition the self-attention block (shown in Figure 6b). The key ( $K$ ), query ( $Q$ ), and value ( $V$ ) matrices can be partitioned in a column-parallel fashion. The output linear layer can then directly operate on the partitioned output of the attention operation (weight matrix partitioned across rows).

This approach splits GEMMs in the MLP and self-attention blocks across GPUs while requiring only two all-reduce operations in the forward pass ( $g$  operator) and two all-reduces in the backward pass ( $f$  operator). We implemented  $f$  and  $g$  in a few lines of code.

### 3 PERFORMANCE ANALYSIS OF PARALLELIZATION CONFIGURATIONS

In this section, we consider the performance implications of combining pipeline and tensor model parallelism with data parallelism; this can be thought of as a three-dimensional parallelization space. Given a fixed budget of GPUs and batch size, one can use different degrees of these parallelism types to train models; each dimension exposes tradeoffs between memory footprint, device utilization, and amount of communication.

We discuss these tradeoffs in the rest of this section, and then show empirical results in §5.3. We present analytical models where relevant for the pipeline bubble size. We qualitatively describe how

communication time behaves; we do not present cost models for communication, however, since all-to-all communication (especially in a hierarchical network topology where interconnects between GPUs on the same server have higher bandwidth than interconnects between servers) is hard to model. To the best of our knowledge, this is the first work to analyze the performance of these parallelization dimensions in a joint way.

#### 3.1 Notation

We use the following notation in this section:

- $(p, t, d)$ : The parallelization dimensions.  $p$  for the pipeline-model-parallel size,  $t$  for the tensor-model-parallel size, and  $d$  for the data-parallel size.
- $n$ : The number of GPUs. We require  $p \cdot t \cdot d = n$ .
- $B$ : The global batch size (provided as input).
- $b$ : The microbatch size.
- $m$ : The number of microbatches in a batch *per pipeline*. Computed as  $\frac{1}{b} \cdot \frac{B}{d}$ .

#### 3.2 Tensor and Pipeline Model Parallelism

Tensor and pipeline model parallelism can both be used to partition a model’s parameters over multiple GPUs. As stated earlier, using pipeline parallelism with periodic flushes results in a pipeline bubble of size  $(p - 1)/m$ . Let us assume that  $d = 1$  (data-parallel size); consequently,  $t \cdot p = n$ . The pipeline bubble size in terms of  $t$  is:

$$\frac{p - 1}{m} = \frac{n/t - 1}{m}.$$

As  $t$  increases, the pipeline bubble thus decreases for fixed  $B$ ,  $b$ , and  $d$  ( $m = B/(b \cdot d)$  is fixed as well).

The amount of communication performed between different GPUs is also affected by the values of  $p$  and  $t$ . Pipeline model parallelism features cheaper point-to-point communication. Tensor model parallelism, on the other hand, uses all-reduce communication that becomes impractical across multi-GPU nodes. Thus, when  $t$  is larger than the number of GPUs in a single node, the overhead of performing all-reduce communication across slower inter-node links slows down the entire end-to-end computation.

**Takeaway #1:** When considering different forms of model parallelism, tensor model parallelism should be used up to degree  $g$  when using  $g$ -GPU servers, and then pipeline model parallelism can be used to scale up to even larger models.

We show results to this effect in §5.3.

#### 3.3 Data and Model Parallelism

We also want to consider the interaction between data and the two types of model parallelism. In this section, we consider these interactions independently for simplicity.

**3.3.1 Pipeline Model Parallelism.** Let  $t = 1$  (tensor-model-parallel size). The number of microbatches per pipeline is  $m = B/(d \cdot b) = b'/d$ , where  $b' := B/b$ . With total number of GPUs  $n$ , the number of pipeline stages is  $p = n/(t \cdot d) = n/d$ . The pipeline bubble size is:

$$\frac{p - 1}{m} = \frac{n/d - 1}{b'/d} = \frac{n - d}{b'}.$$



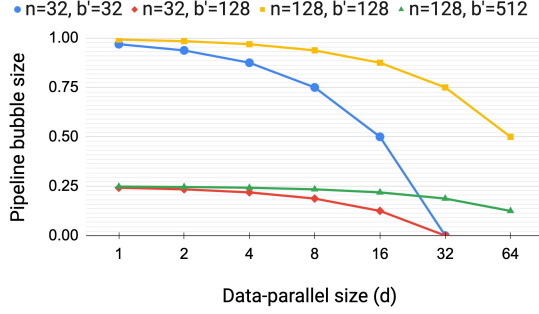


Figure 7: Fraction of time spent idling due to pipeline flush (pipeline bubble size) versus data-parallel size ( $d$ ), for different numbers of GPUs ( $n$ ) and ratio of batch size to microbatch size ( $b' = B/b$ ).

As  $d$  becomes larger,  $n - d$  becomes smaller, and thus the pipeline bubble becomes smaller. Figure 7 shows the behavior of the pipeline bubble size for various values of  $d$ ,  $n$ , and  $b'$ . It might not be possible to increase  $d$  all the way to  $n$  for all models, since models might be larger than the memory capacity of a single accelerator.

Overall throughput will thus increase if the all-reduce communication needed for data parallelism does not drastically increase with higher  $d$ , which should hold since the communication time for a ring-based implementation scales with  $\frac{d-1}{d}$ .

We can also analyze the impact of increasing the batch size  $B$ . For a given parallel configuration, as the batch size  $B$  increases,  $b' = B/b$  increases,  $(n - d)/b'$  decreases, consequently increasing throughput. All-reduce communication required by data parallelism also becomes more infrequent, further increasing throughput.

**3.3.2 Data and Tensor Model Parallelism.** With tensor model parallelism, all-reduce communication needs to be performed for *every* microbatch. This can be expensive across multi-GPU servers. On the other hand, data parallelism only needs to perform expensive all-reduce communication (in the form of an all-reduction) *once per batch*. Moreover, with tensor model parallelism, each model-parallel rank performs a subset of the computation in each model layer, and thus for insufficiently-large layers, modern GPUs might not perform these sub-matrix computations with peak efficiency.

**Takeaway #2:** When using data and model parallelism, a total model-parallel size of  $M = t \cdot p$  should be used so that the model’s parameters and intermediate metadata fit in GPU memory; data parallelism can be used to scale up training to more GPUs.

### 3.4 Microbatch Size

The choice of the microbatch size  $b$  also affects model-training throughput. For example, we see in Figure 8 that per-GPU throughput increases by up to 1.3× with a larger microbatch size on a single GPU. We now want to determine the optimal microbatch size  $b$  given a parallel configuration ( $p, t, d$ ) and batch size  $B$ . The amount of data-parallel communication will be the same regardless of the microbatch size. Let us assume that we have functions  $t_f(b)$  and  $t_b(b)$  that map the microbatch size to the forward and backward computation times for a single microbatch. As before, define  $b'$  as  $B/d$ . The total time spent computing a batch, ignoring

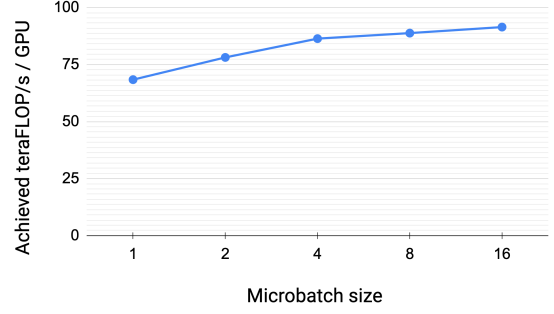


Figure 8: Per-GPU throughput versus microbatch size for a GPT model with a billion parameters (128 attention heads, hidden size of 4096, 4 transformer layers).

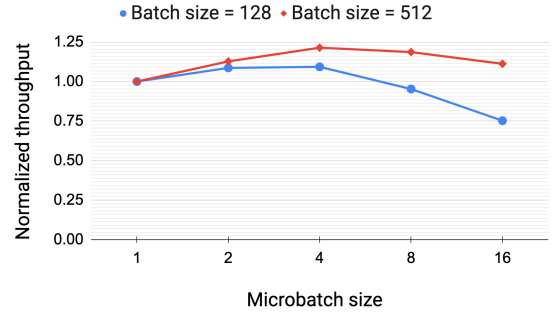


Figure 9: Behavior of theoretical throughput (time computed as  $t = (b'/b + p - 1) \cdot (t_f(b) + t_b(b))$ ) with respect to the microbatch size  $b$  for the GPT model with a billion parameters (128 attention heads, hidden size of 4096, 4 transformer layers), using two batch sizes.

communication cost, is then:

$$(b'/b + p - 1) \cdot (t_f(b) + t_b(b)).$$

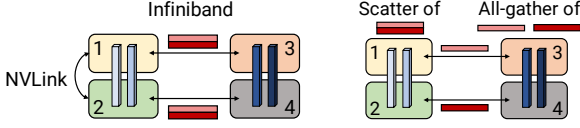
Figure 9 shows the behavior of this function for a GPT model with a billion parameters (we show normalized time with respect to microbatch size 1 for the two batch sizes) on a single GPU with  $(p, t) = (8, 8)$ . The optimal  $b$  for both batch sizes is 4, with higher performance with the larger batch size.

**Takeaway #3:** The optimal microbatch size  $b$  depends on the throughput and memory footprint characteristics of the model, as well as the pipeline depth  $p$ , data-parallel size  $d$ , and batch size  $B$ .

### 3.5 Activation Recomputation

Activation recomputation[9, 14–16] is an optional technique that trades off an increase in the number of compute operations performed for additional memory footprint, by running the forward pass a second time just before the backward pass (and stashing only the input activations for a given pipeline stage, as opposed to the entire set of intermediate activations, which is much larger). This lowered memory footprint can provide two benefits:

- Ability to train large models.
- Increase in net throughput despite increasing number of compute operations by  $\sim 33\%$  by facilitating higher per-GPU microbatch sizes, which improve single-GPU utilization.



(a) W/o scatter/gather optimization. (b) With scatter/gather optimization.

**Figure 10: Scatter/gather communication optimization.** Light blue blocks are layers in the first pipeline stage, and dark blue blocks are layers in the second pipeline stage. Without the scatter/gather optimization, the same tensor is sent redundantly over inter-node InfiniBand links. Instead, at the sender, we can scatter the tensor into smaller chunks, reducing the sizes of tensors sent over InfiniBand links. The final tensor can then be rematerialized at the receiver using all-gather over NVLink.

Previous work like PipeDream-2BW [23] has looked at the performance impact of using activation recomputation. Activation recomputation is required to train reasonably large models with pipeline parallelism to keep memory footprint acceptably low.

## 4 IMPLEMENTATION

We implemented pipeline parallelism on top of the Megatron codebase [2], which already supported tensor model parallelism and data parallelism. Our code is implemented in PyTorch [24]. We use NCCL [4] for communication between devices. To obtain good performance, we implemented optimizations targeting both communication and computation, which we outline below.

### 4.1 Communication Optimizations

When using pipeline parallelism, we want to send and receive tensors in the forward and backward direction in parallel. Each DGX A100 is equipped with 8 InfiniBand (IB) networking cards. Unfortunately, sends and receives are point-to-point, and only happen between a pair of GPUs on two servers, making it hard to leverage all 8 cards for a single communication call within the pipeline.

However, we can leverage the fact that we use both tensor model parallelism and pipeline model parallelism to reduce the overhead of cross-node communication. In particular, we note that the output of each transformer layer is replicated (after  $g$  in MLP block) across the tensor-parallel ranks (Figure 6a). As a result, ranks in two consecutive pipeline stages that are performing tensor model parallelism send and receive the exact same set of tensors (Figure 10a).

For large enough models, we use a tensor-model-parallel size of 8. This means we are sending the same set of tensors 8 times between corresponding GPUs on adjacent multi-GPU servers. To reduce this redundancy, we can instead split the tensor on the send side into equal-sized chunks, and then only send the chunk to the corresponding rank on the next node using its own InfiniBand card (e.g., rank 1 sends to rank 3 and rank 2 sends to rank 4 in Figure 17). With 8 tensor-model-parallel ranks, each chunk would be one-eighth smaller. Then, on the receiver side, we can perform an all-gather over NVLink, which is much faster than the InfiniBand interconnect, to re-materialize the full tensor. This is shown in Figure 10b. We call this the *scatter/gather communication optimization*. This optimization helps better leverage the multiple IB cards on

the DGX A100 servers, and makes more communication-intensive schedules such as the interleaved one feasible.

## 4.2 Computation Optimizations

We implemented three model-specific optimizations to the computational graph to attain high performance. First, we changed the data layout in the transformer layer to avoid memory-intensive transpose operations, and to enable the use of strided batched GEMM kernels. Specifically, we changed the data layout from  $[b, s, a, h]$  to  $[s, b, a, h]$ , where  $b$ ,  $s$ ,  $a$ , and  $h$  are batch, sequence, attention-head, and hidden-size dimensions, respectively. Second, we generated fused kernels for a sequence of element-wise operations (bias + GeLU and bias + dropout + add) using PyTorch JIT [6]. Third, we created two custom kernels to enable the fusion of scale, mask, and softmax (reduction) operations: one to support general masking (used in models such as BERT) and another to support implicit casual masking (used in auto-regressive models such as GPT).

## 5 EVALUATION

In this section, we seek to answer the following questions:

- How well does the combination of pipeline and tensor model parallelism along with data parallelism perform? Does the resulting performance result in realistic end-to-end training times?
- How well does pipeline parallelism scale for a given model and batch size? How much impact does the interleaved schedule have on performance?
- How do different parallelization dimensions compose with each other? What is the impact of hyperparameters such as microbatch size?
- What is the impact of the scatter-gather communication optimization? What types of limits do we put on hardware when running training iterations at scale?

All of our results are run with 16-bit precision in NVIDIA’s Selene cluster [7]. Each cluster node has 8 NVIDIA 80-GB A100 GPUs [3], connected to each other by NVLink and NVSwitch [5]. Each node has eight NVIDIA Mellanox 200Gbps HDR InfiniBand HCAs for application communication, with an additional two HCAs per node for dedicated storage. The nodes are connected in a fat-tree topology with 850 switches. The cluster uses an all-NVME shared parallel filesystem for high-performance data access and storage. The peak device throughput of an A100 GPU with 16-bit precision is 312 teraFLOP/s. For most of our results, we report throughput per GPU; total aggregate throughput can be computed by multiplying with the number of GPUs used.

For our microbenchmarks, we use GPT models of appropriate sizes. In particular, the model needs to fit on the number of model-parallel GPUs used in the experiment. We use standard model architectures such as GPT-3 [8] when appropriate.

### 5.1 End-to-End Performance

We consider the end-to-end performance of our system on GPT models ranging from a billion to a trillion parameters, using tensor, pipeline, and data parallelism (degrees picked using heuristics described in §3). In particular, we use the interleaved pipeline schedule with the scatter/gather optimization enabled. All models use a

Model size	Hidden size	Number of layers	Number of parameters (billion)	Model-parallel size	Number of GPUs	Batch size	Achieved teraFLOP/s per GPU	Percentage of theoretical peak FLOP/s	Achieved aggregate petaFLOP/s
1.7B	2304	24	1.7	1	32	512	137	44%	4.4
3.6B	3072	30	3.6	2	64	512	138	44%	8.8
7.5B	4096	36	7.5	4	128	512	142	46%	18.2
18B	6144	40	18.4	8	256	1024	135	43%	34.6
39B	8192	48	39.1	16	512	1536	138	44%	70.8
76B	10240	60	76.1	32	1024	1792	140	45%	143.8
145B	12288	80	145.6	64	1536	2304	148	47%	227.1
310B	16384	96	310.1	128	1920	2160	155	50%	297.4
530B	20480	105	529.6	280	2520	2520	163	52%	410.2
1T	25600	128	1008.0	512	3072	3072	163	52%	502.0

Table 1: Weak scaling throughput for GPT models ranging from 1 billion to 1 trillion parameters.

vocabulary size (denoted by  $V$ ) of 51,200 (multiple of 1024) and a sequence length ( $S$ ) of 2048. We vary hidden size ( $h$ ), number of attention heads, and number of layers ( $l$ ). The number of parameters in a model,  $P$ , can be computed as:

$$P = 12lh^2 \left(1 + \frac{13}{12h} + \frac{V+S}{12lh}\right). \quad (1)$$

As the model size increases, we also increase the batch size ( $B$ ) and the number of GPUs ( $n$ ). The majority of floating-point operations in the model are performed in the matrix multiplications (GEMMs) in the transformer and logit layers. Considering just these GEMMs, the number of floating-point operations per iteration (see Appendix for more details) can be computed as:

$$F = 96BSlh^2 \left(1 + \frac{S}{6h} + \frac{V}{16lh}\right). \quad (2)$$

This is a lower bound for the true FLOP count but should be close to the actual value. We count a FLOP as a floating-point operation regardless of precision. We note that equation (2) assumes activation recomputation and takes into account an extra forward pass.

Table 1 shows the model configurations along with the achieved FLOP/s (both per GPU and aggregate over all GPUs). We see super-linear scaling to 3072 A100 GPUs (384 DGX A100 nodes), since GPU utilization improves as the models get larger (larger matrix multiplications) without significant increase in the communication time relative to computation time. Note that throughput is measured for end-to-end training, i.e., includes all operations including data loading, optimization, communication, and logging. Our largest case achieves 52% of peak device throughput, and our smallest case achieves 44% of peak device throughput.

**Training Time Estimates.** Given these throughputs, we can also estimate the total amount of time needed for end-to-end training on  $T$  tokens. Training requires  $I = T/(B \cdot S)$  iterations. Using the value of  $F$  from equation (2) and empirical end-to-end throughputs from Table 1, we can estimate total training time.

We note that for the configurations in Table 1, we have  $6h \gg S$ ,  $16lh \gg (V+S)$ , and  $12lh \gg V$ . Combining these observations with

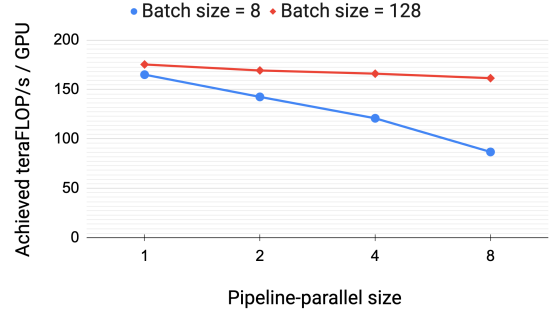


Figure 11: Throughput per GPU of pipeline parallelism using two different batch sizes in a weak-scaling experiment setup (model size increases with the pipeline-parallel size).

equations (1) and (2), we arrive at:

$$\text{Training time (seconds)} \approx \frac{8TP}{nX}. \quad (3)$$

Let us consider the GPT-3 model with  $P=175$  billion parameters as an example. This model was trained on  $T=300$  billion tokens. On  $n=1024$  A100 GPUs using batch-size 1536, we achieve  $X=140$  teraFLOP/s per GPU. As a result, the time required to train this model can be estimated as:

$$\text{GPT-3 training time} \approx \frac{8 \times 300 \times 10^9 \times 175 \times 10^9}{1024 \times 140 \times 10^{12}} \approx 34 \text{ days,}$$

just over a month.

For the 1 trillion parameter model, assume that we need about 450 billion tokens for end-to-end training. With 3072 A100 GPUs, we can achieve a per-GPU throughput of 163 petaFLOP/s. Thus, end-to-end training time will be around 84 days, or about 3 months.

## 5.2 Pipeline Parallelism

We now evaluate the weak-scaling performance of pipeline parallelism in isolation, and also compare the performance of the non-interleaved schedule to the interleaved schedule.



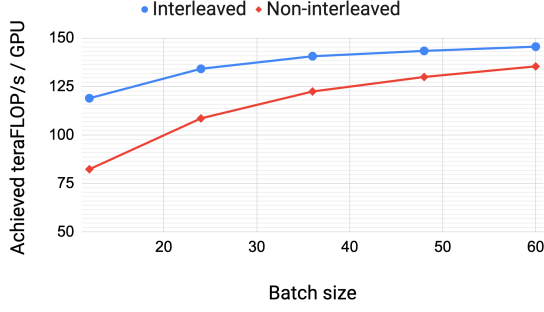


**Figure 12: Throughput per GPU of interleaved and non-interleaved schedules for a GPT model with 175 billion parameters using 96 A100 GPUs.**

**5.2.1 Weak Scaling.** We evaluate the scaling of the default non-interleaved pipeline-parallel schedule using a weak scaling setup, a GPT model with 128 attention heads and a hidden size of 20480, and a microbatch size of 1. As we increase the number of pipeline stages, we also increase the size of the model by proportionally increasing the number of layers in the model, e.g., with a pipeline-parallel size of 1, we use a model with 3 transformer layers and 15 billion parameters, and with a pipeline-parallel size of 8, we use a model with 24 transformer layers and 121 billion parameters. We use a tensor-parallel size of 8 for all configurations, and vary the total number of A100 GPUs used from 8 to 64. Figure 11 shows throughput per GPU for two different batch sizes to illustrate the impact of the pipeline bubble, which behaves as  $\frac{p-1}{m}$  (§2.2.1). As expected, the higher batch size scales better since the pipeline bubble is amortized over more microbatches.

**5.2.2 Interleaved versus Non-Interleaved Schedule.** Figure 12 shows the per-GPU-throughput for interleaved and non-interleaved schedules on a GPT model with 175 billion parameters (96 layers, 96 attention heads, hidden size of 12288). The interleaved schedule with the scatter/gather communication optimization has higher computational performance than the non-interleaved (default) schedule. This gap closes as the batch size increases due to two reasons: (a) as the batch size increases, the bubble size in the default schedule decreases, (b) the amount of point-to-point communication within the pipeline is proportional to the batch size, and consequently the non-interleaved schedule catches up as the amount of communication increases. Without the scatter/gather optimization, the default schedule performs better than the interleaved schedule at larger batch sizes (not shown).

### 5.3 Comparison of Parallel Configurations

In this sub-section, we show the various tradeoffs associated with combining different parallelization dimensions. In particular, we show the performance for parallel configurations using the same number of GPUs for a given model and multiple batch sizes.

**5.3.1 Tensor versus Pipeline Parallelism.** We evaluate the impact of pipeline and tensor model parallelism on performance for a given model and batch size. The empirical results in Figure 13 show the importance of using both tensor and pipeline model parallelism in

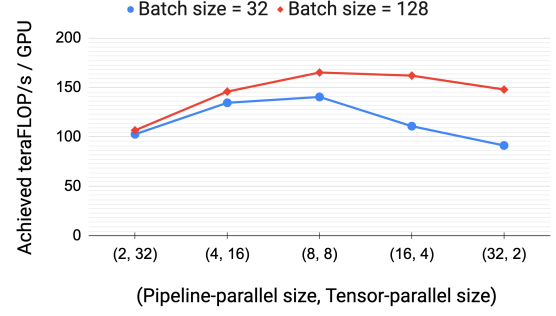


**Figure 13: Throughput per GPU of various parallel configurations that combine pipeline and tensor model parallelism using a GPT model with 162.2 billion parameters, two different batch sizes, and 64 A100 GPUs.**

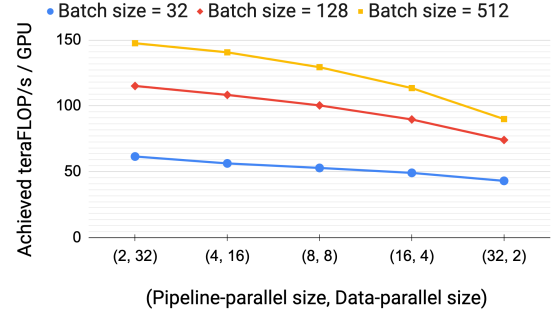


**Figure 14: Throughput per GPU of various parallel configurations that combine data and pipeline model parallelism using a GPT model with 5.9 billion parameters, three different batch sizes, microbatch size of 1, and 64 A100 GPUs.**

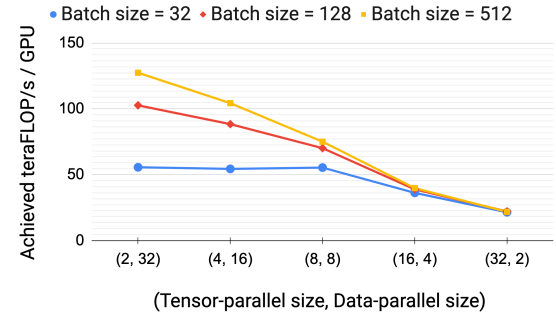


**Figure 15: Throughput per GPU of various parallel configurations that combine data and tensor model parallelism using a GPT model with 5.9 billion parameters, three different batch sizes, microbatch size of 1, and 64 A100 GPUs.**

conjunction to train a 161-billion-parameter GPT model (32 transformer layers to support pipeline-parallel size of 32, 128 attention heads, hidden size of 20480) with low communication overhead and high compute resource utilization. We observe that tensor model parallelism is best within a node (DGX A100 server) due to its expensive all-reduce communication. Pipeline model parallelism, on the other hand, uses much cheaper point-to-point communication that

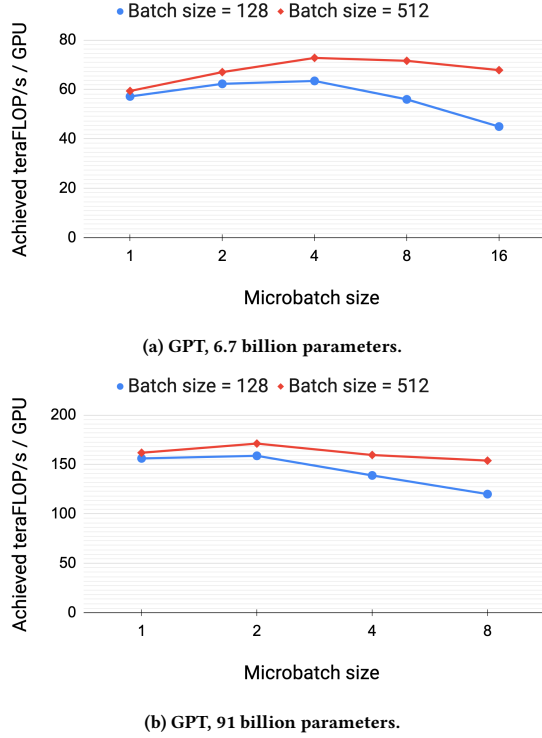


Figure 16: Throughput per GPU of a given parallel configuration for different microbatch sizes, for two different batch sizes using 64 A100 GPUs.

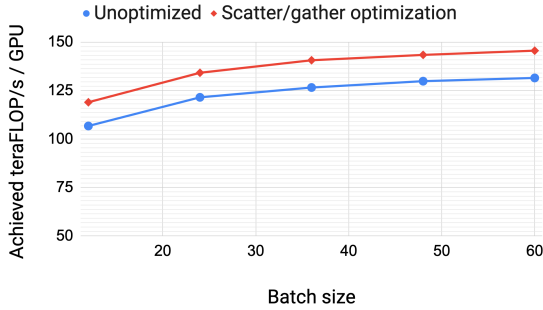


Figure 17: Throughput per GPU with and without the scatter/gather optimization for a GPT model with 175 billion parameters using 96 A100 GPUs and the interleaved schedule.

can be performed across nodes without bottlenecking the entire computation. However, with pipeline parallelism, significant time can be spent in the pipeline bubble: the total number of pipeline stages should thus be limited so that the number of microbatches in the pipeline is a reasonable multiple of the number of pipeline stages. Consequently, we see peak performance when the tensor-parallel size is equal to the number of GPUs in a single node (8 with DGX A100 nodes). This result indicates that neither tensor model parallelism (used by Megatron [31]) nor pipeline model parallelism (used by PipeDream [23] and others) in isolation can match the performance of using both techniques in conjunction.

**5.3.2 Pipeline versus Data Parallelism.** We evaluate the impact of data and pipeline model parallelism on performance for a GPT model with 5.9 billion parameters (32 transformer layers, 32 attention heads, hidden size of 3840) in Figure 14. We use a smaller model than before since we want to show performance for models that fit when the model-parallel size is only 2. For simplicity, we keep the microbatch size equal to 1 in these experiments. We see that for each batch size, the throughput decreases as the pipeline-parallel size increases, matching our analytical model from §3.3. Pipeline model parallelism should be used primarily to support the training of large models that do not fit on a single worker, and data parallelism should be used to scale up training.

**5.3.3 Tensor versus Data Parallelism.** We also evaluate the impact of data and tensor model parallelism on performance for the same GPT model with 5.9 billion parameters in Figure 15 (smaller model used for same reason as above). As before, we keep the microbatch size equal to 1 initially. With larger batch sizes and a microbatch size of 1, data-parallel communication is infrequent; the all-to-all communication required in tensor model parallelism needs to be performed for *every* microbatch in a batch. This all-to-all communication with tensor model parallelism dominates end-to-end training time, especially when communication needs to be performed across multi-GPU nodes. Additionally, as the tensor-model-parallel size increases, we perform smaller matrix multiplications on every GPU, decreasing utilization on each GPU.

We should note that although data parallelism is more efficient, for very large models with a limited training batch size (which is the case for most language models), we cannot only use data parallelism because of a) insufficient memory capacity, and b) scaling limitations of data parallelism due to limited batch size.

## 5.4 Microbatch Size

We evaluate the impact of the microbatch size on the performance of parallel configurations that combine pipeline and tensor model parallelism in Figure 16 for two different model sizes  $((t, p) = (8, 8))$ . The effect of microbatch size on throughput is *model-dependent*: we see that the best microbatch size is 4 for the smaller 6.7-billion-parameter model (with smaller hidden size), and 2 for the larger 91-billion-parameter model. For a given batch size, increasing the microbatch size decreases the number of microbatches in the pipeline ( $m$ ), leading to a larger pipeline bubble; however, increasing the microbatch size can also improve GPU utilization by increasing the arithmetic intensity of executed kernels. These two factors are at odds with each other, which makes the choice of optimal microbatch size challenging. Our analytical model from §3.3 reasonably approximates true performance, and can be used as a proxy to determine how to pick this hyperparameter value for various models and training configurations.

## 5.5 Scatter-Gather Optimization

Figure 17 shows per-GPU-throughput with and without (unoptimized) the scatter/gather communication optimization for the GPT-3 model with 175 billion parameters. We see an improvement of up to 11% in end-to-end throughput for communication-intensive schedules (large batch size with interleaving). This highlights the

importance of the DGX A100’s 8 InfiniBand cards in achieving high training throughput.

## 5.6 Inter-Node Communication Bandwidth

Our strong results are a byproduct of using an optimized software and hardware stack *together*. In particular, we take advantage of the high-bandwidth communication links between GPUs on the same server and across servers. On the trillion-parameter-model with 3072 GPUs, we observed that the effective bisection bandwidth of point-to-point communication among pipeline stages is 892 GB/s, while the effective bisection bandwidth of all-reduce operations among data-parallel replicas is 12.9 TB/s. A less-optimized partitioning of operators across devices would lead to more inter-node communication, hampering scaling performance.

## 5.7 Checkpoint Loading and Saving

An important practical consideration for the training of large models is loading and saving model checkpoints, which are especially large for the models considered in this paper. For example, the trillion-parameter model has a checkpoint of size 13.8 terabytes. Fortunately, our on-premise cluster has a high-performance parallel filesystem that helps us sustain the required read and write bandwidth to efficiently load and save these checkpoints. The initial load of checkpoints for the trillion-parameter model by all 384 nodes (3072 GPUs) reaches 100% of peak read bandwidth (1TB/s), achieving the maximum read throughput possible from the parallel filesystem. Checkpoint saves from rank 0 of data-parallel groups reaches 40% of peak write bandwidth (273 GB/s).

## 6 RELATED WORK

In this section, we discuss techniques to train models at scale that have not yet been discussed at length in this paper.

**Combination of Model and Parallelism.** Pipeline parallelism is a common technique used to train large models. Pipeline parallelism comes in a few flavors: the mode discussed in this paper uses flushes to ensure *exact* strict optimizer semantics. TeraPipe [20] exposes fine-grained pipeline parallelism across tokens in a single training sequence for auto-regressive models like GPT. There are other ways of implementing pipeline parallelism with relaxed semantics: PipeDream-2BW [23] maintains two weight versions and guarantees 1-stale weight updates without expensive flushes, while PipeMare [35] and Kosson et al. [18] use asynchronous pipeline parallelism. These techniques all have improved throughput compared to the techniques with pipeline flushes considered in this paper, but potentially at the cost of convergence rate or final accuracy. Moreover, pipeline parallelism in isolation can still only scale to a number of devices equal to the number of layers in the model, which is limiting for certain types of model architectures.

DeepSpeed [1] combined pipeline parallelism with tensor and data parallelism to train models with up to a trillion parameters, but with lower throughput than what was shown in this paper (502 petaFLOP/s vs. 37 petaFLOP/s) for a few reasons: operator fusion to keep most of the operator graph compute-bound, a more-efficient pipeline parallelism schedule minimize the pipeline bubble size, fast hardware (A100 vs. V100 GPUs and high-bandwidth links between GPUs on the same and different servers), and scaling to more GPUs.

Mesh-TensorFlow [30] proposes a language for easily specifying parallelization strategies that combine data and model parallelism.

**CPU Offloading.** Another way to train large models is to offload “non-active” parameters to the CPU, as in ZeRO-Offload [29]. While this makes it possible to train large models on a fewer number of resources, it does not increase training throughput, meaning training of large models can take impractically long.

**Sharded Data Parallelism.** Another method to train large models is to use ZeRO’s sharded data parallelism [28]. As with vanilla data parallelism, every worker operates on different inputs. Optimizer state (e.g., first and second moments of gradients for the Adam optimizer), weight parameters, and weight gradients are partitioned across workers. Workers fetch relevant state from their “owning” workers as inputs are processed (e.g., the first shard of weight parameters needs to be fetched from worker 0 by *all* workers before running the forward pass on each worker) – this results in scatter/gather-style communication patterns.

**Automatic Partitioning and Cost Modeling of Communication.** FlexFlow [17], PipeDream [22], Tarnawski et al. [32], and DAPPLE [11] all auto-partition model training graphs over multiple devices. However, each of these do not consider all the parallelism dimensions considered in this paper: pipeline and tensor model parallelism, data parallelism, microbatch size, and the effect of memory-savings optimizations like activation recomputation on the training of models larger than the memory capacity of a single accelerator. Gholami et al. [12] show how communication costs for combinations of data and model parallelism can be modeled.

**HPC for Model Training.** Goyal et al. [13] and You et al. [37] both looked at how to use High Performance Computing techniques to train highly-accurate ImageNet models in minutes. However, the image classification models considered fit comfortably on a single accelerator, rendering model parallelism unnecessary, and also support very large batch sizes (> 32k) that allow scaling data parallelism to large worker counts with infrequent communication.

## 7 DISCUSSION AND CONCLUSION

In this paper, we have showed how different parallelization strategies (intra-node tensor model parallelism, inter-node pipeline model parallelism and data parallelism) can be composed to achieve high aggregate throughput (502 petaFLOP/s) while training large models with a trillion parameters. We discussed the various tradeoffs associated with each of these types of parallelism, and how the interactions between them need to be considered carefully when they are combined.

Going forward, we want to further optimize our pipelining schedules: for example, we expect a throughput improvement if we are able to compute data gradients before weight gradients (since tensors can be sent upstream earlier, leading to a cheaper pipeline flush). We also want to evaluate these techniques on other types of model architectures, e.g., DLRM models for recommendation. Finally, we want to actually train models to convergence, and better understand the implications of using schedules without pipeline flushes (such as PipeDream-2BW) which relax weight update semantics for higher throughput.

## REFERENCES

- [1] DeepSpeed: Extreme-Scale Model Training for Everyone. <https://www.microsoft.com/en-us/research/blog/deepspeed-extreme-scale-model-training-for-everyone/>.
- [2] Megatron Repository. <https://github.com/nvidia/megatron-lm>.
- [3] NVIDIA A100 Tensor Core GPU. <https://www.nvidia.com/en-us/data-center/a100/>.
- [4] NVIDIA Collective Communication Library (NCCL). <https://developer.nvidia.com/nccl>.
- [5] NVLink and nVSwitch. <https://www.nvidia.com/en-us/data-center/nvlink/>.
- [6] PyTorch JIT. <https://pytorch.org/docs/stable/jit.html>.
- [7] Selene. <https://www.top500.org/system/179842/>.
- [8] Tom Brown, Benjamin Mann, Nick Ryder, Melanie Subbiah, and et al. Language Models are Few-Shot Learners. *arXiv preprint arXiv:2005.14165*, 2020.
- [9] Tianqi Chen, Bing Xu, Chiyuan Zhang, and Carlos Guestrin. Training Deep Nets with Sublinear Memory Cost. *arXiv preprint arXiv:1604.06174*, 2016.
- [10] Jacob Devlin, Ming-Wei Chang, Kenton Lee, and Kristina Toutanova. Bert: Pre-training of Deep Bidirectional Transformers for Language Understanding. *arXiv preprint arXiv:1810.04805*, 2018.
- [11] Shiqing Fan, Yi Rong, Chen Meng, Zongyan Cao, Siyu Wang, Zhen Zheng, Chuan Wu, Guoping Long, Jun Yang, Lixue Xia, et al. DAPPLE: A Pipelined Data Parallel Approach for Training Large Models. In *Proceedings of the 26th ACM SIGPLAN Symposium on Principles and Practice of Parallel Programming*, pages 431–445, 2021.
- [12] Amir Gholami, Arifur Azad, Peter Jin, Kurt Keutzer, and Aydin Buluc. Integrated Model, Batch, and Domain Parallelism in Training Neural Networks. In *Proceedings of the 30th on Symposium on Parallelism in Algorithms and Architectures*, pages 77–86, 2018.
- [13] Priya Goyal, Piotr Dollár, Ross Girshick, Pieter Noordhuis, Lukasz Wesolowski, Aapo Kyrola, Andrew Tulloch, Yangqing Jia, and Kaiming He. Accurate, Large Minibatch SGD: Training ImageNet in 1 Hour. *arXiv preprint arXiv:1706.02677*, 2017.
- [14] Andreas Griewank and Andrea Walther. Revolve: An Implementation of Checkpointing for the Reverse or Adjoint Mode of Computational Differentiation. *ACM Transactions on Mathematical Software (TOMS)*, 26(1):19–45, 2000.
- [15] Yanping Huang, Youlong Cheng, Ankur Bapna, Orhan Firat, Dehao Chen, Mia Chen, Hyukjoong Lee, Jiquan Ngiam, Quoc V Le, Yonghui Wu, et al. GPipe: Efficient Training of Giant Neural Networks using Pipeline Parallelism. In *Advances in Neural Information Processing Systems*, pages 103–112, 2019.
- [16] Paras Jain, Ajay Jain, Aniruddha Nrusimha, Amir Gholami, Pieter Abbeel, Joseph Gonzalez, Kurt Keutzer, and Ion Stoica. Breaking the Memory Wall with Optimal Tensor Rematerialization. In *Proceedings of Machine Learning and Systems 2020*, pages 497–511, 2020.
- [17] Zhihao Jia, Matei Zaharia, and Alex Aiken. Beyond Data and Model Parallelism for Deep Neural Networks. In *Proceedings of the 2nd Conference on Machine Learning and Systems (MLSys)*, 2018.
- [18] Atli Kossou, Vitaliy Chiley, Abhinav Venigalla, Joel Hestness, and Urs Köster. Pipelined Backpropagation at Scale: Training Large Models without Batches. *Proceedings of Machine Learning and Systems*, 2021.
- [19] Shen Li, Yanli Zhao, Rohan Varma, Omkar Salpekar, Pieter Noordhuis, Teng Li, Adam Paszke, Jeff Smith, Brian Vaughan, Pritam Damania, et al. PyTorch Distributed: Experiences on Accelerating Data Parallel Training. *arXiv preprint arXiv:2006.15704*, 2020.
- [20] Zhuohan Li, Siyuan Zhuang, Shiyuan Guo, Danyang Zhuo, Hao Zhang, Dawn Song, and Ion Stoica. TeraPipe: Token-Level Pipeline Parallelism for Training Large-Scale Language Models. *arXiv preprint arXiv:2102.07988*, 2021.
- [21] Yinhan Liu, Myle Ott, Naman Goyal, Jingfei Du, Mandar Joshi, Danqi Chen, Omer Levy, Mike Lewis, Luke Zettlemoyer, and Veselin Stoyanov. RoBERTa: A Robustly Optimized BERT Pretraining Approach. *CoRR*, abs/1907.11692, 2019.
- [22] Deepak Narayanan, Aaron Harlap, Amar Phanishayee, Vivek Seshadri, Nikhil R Devanur, Gregory R Ganger, Phillip B Gibbons, and Matei Zaharia. PipeDream: Generalized Pipeline Parallelism for DNN Training. In *Proceedings of the 27th ACM Symposium on Operating Systems Principles*, pages 1–15, 2019.
- [23] Deepak Narayanan, Amar Phanishayee, Kaiyu Shi, Xie Chen, and Matei Zaharia. Memory-Efficient Pipeline-Parallel DNN Training. *arXiv preprint arXiv:2006.09503*, 2020.
- [24] Adam Paszke, Sam Gross, Francisco Massa, Adam Lerer, James Bradbury, Gregory Chanan, Trevor Killeen, Zeming Lin, Natalia Gimelshein, Luca Antiga, Alban Desmaison, Andreas Kopf, Edward Yang, Zachary DeVito, Martin Raison, Alykhan Tejani, Sasank Chilamkurthy, Benoit Steiner, Lu Fang, Junjie Bai, and Soumith Chintala. PyTorch: An Imperative Style, High-Performance Deep Learning Library. In *Advances in Neural Information Processing Systems*, volume 32, 2019.
- [25] Alec Radford, Karthik Narasimhan, Tim Salimans, and Ilya Sutskever. Improving Language Understanding by Generative Pre-Training, 2018.
- [26] Alec Radford, Jeffrey Wu, Rewon Child, David Luan, Dario Amodei, and Ilya Sutskever. Language Models are Unsupervised Multitask Learners. *OpenAI Blog*, 1(8):9, 2019.
- [27] Colin Raffel, Noam Shazeer, Adam Roberts, Katherine Lee, Sharan Narang, Michael Matena, Yanqi Zhou, Wei Li, and Peter J. Liu. Exploring the Limits of Transfer Learning with a Unified Text-to-Text Transformer. *arXiv:1910.10683*, 2019.
- [28] Samyam Rajbhandari, Jeff Rasley, Olatunji Ruwase, and Yuxiong He. ZeRO: Memory Optimization Towards Training A Trillion Parameter Models. *arXiv preprint arXiv:1910.02054*, 2019.
- [29] Jie Ren, Samyam Rajbhandari, Reza Yazdani Aminabadi, Olatunji Ruwase, Shuangyan Yang, Minjia Zhang, Dong Li, and Yuxiong He. ZeRO-Offload: Democratizing Billion-Scale Model Training. *arXiv preprint arXiv:2101.06840*, 2021.
- [30] Noam Shazeer, Youlong Cheng, Niki Parmar, Dustin Tran, Ashish Vaswani, Penporn Koanantakool, Peter Hawkins, Hyukjoong Lee, Mingsheng Hong, Cliff Young, Ryan Sepassi, and Blake Hechtman. Mesh-TensorFlow: Deep Learning for Supercomputers. In *Neural Information Processing Systems*, 2018.
- [31] Mohammad Shoeybi, Mostofa Patwary, Raul Puri, Patrick LeGresley, Jared Casper, and Bryan Catanzaro. Megatron-LM: Training Multi-Billion Parameter Language Models using GPU Model Parallelism. *arXiv preprint arXiv:1909.08053*, 2019.
- [32] Jakub M Tarnawski, Amar Phanishayee, Nikhil Devanur, Divya Mahajan, and Fanny Nina Paravecino. Efficient Algorithms for Device Placement of DNN Graph Operators. In *Advances in Neural Information Processing Systems*, pages 15451–15463, 2020.
- [33] Ashish Vaswani, Noam Shazeer, Niki Parmar, Jakob Uszkoreit, Llion Jones, Aidan N Gomez, Lukasz Kaiser, and Illia Polosukhin. Attention is All You Need. *arXiv preprint arXiv:1706.03762*, 2017.
- [34] Eric P Xing, Qirong Ho, Wei Dai, Jin Kyu Kim, Jinliang Wei, Seunghak Lee, Xun Zheng, Pengtao Xie, Abhimanu Kumar, and Yaoliang Yu. Petuum: A New Platform for Distributed Machine Learning on Big Data. *IEEE Transactions on Big Data*, 1(2):49–67, 2015.
- [35] Bowen Yang, Jian Zhang, Jonathan Li, Christopher Ré, Christopher Aberger, and Christopher De Sa. PipeMare: Asynchronous Pipeline Parallel DNN Training. *Proceedings of Machine Learning and Systems*, 2021.
- [36] Zhilin Yang, Zihang Dai, Yiming Yang, Jaime G. Carbonell, Ruslan Salakhutdinov, and Quoc V. Le. XLNet: Generalized Autoregressive Pretraining for Language Understanding. *CoRR*, abs/1906.08237, 2019.
- [37] Yang You, Zhao Zhang, Cho-Jui Hsieh, James Demmel, and Kurt Keutzer. ImageNet Training in Minutes. In *Proceedings of the 47th International Conference on Parallel Processing*, pages 1–10, 2018.

## A FLOATING-POINT OPERATIONS

In this section, we describe how we calculate the number of floating-point operations in a model. As before, consider a language model with  $l$  transformer layers, hidden size  $h$ , sequence length  $S$ , vocabulary size  $V$ , and training batch size  $B$ . We assume that the MLP part of the transformer layer uses a hidden size of  $4h$ . Additionally, we use activation recomputation, and assume that the main contributors to the number of floating-point operations are the matrix multiplications (GEMMs) in the transformer and logit layer. This is a lower bound for the true FLOP count but should be close to the actual value. We count a FLOP as a floating-point operation regardless of precision. Concretely, a matrix multiplication  $A_{m \times k} \times X_{k \times n}$  in 16-bit precision results in  $2m \times k \times n$  FLOPs (factor of 2 is needed to account for multiplies and adds).

A transformer layer consists of an attention block followed by a 2-layer feed-forward network. For the attention block, the main contributors to floating-point operations are: key, query, and value transformation ( $6BS^2h^2$  operations), attention matrix computation ( $2BS^2h$  operations), attention over values ( $2BS^2h$  operations), and post-attention linear projection ( $2BS^2h^2$  operations). For the feed-forward network that increases the hidden size to  $4h$  and then reduces it back to  $h$ , we have  $16BS^2h^2$  floating-point operations.

Summing these together, each transformer layer results in  $24BS^2h^2 + 4BS^2h$  FLOPs for the forward pass. The backward pass requires double the number of FLOPs since we need to calculate the gradients with respect to both input and weight tensors. In addition, we are

using activation recomputation, which requires an additional forward pass before the backward pass. As a result, the total number of floating-point operations required per transformer layer is:

$$4 \times (24BS^2h^2 + 4BS^2h) = 96BS^2h^2(1 + \frac{S}{6h}).$$

The other main contributor to the number of floating-point operations is the logits layer in the language model head, which transforms features of dimension  $h$  to the vocabulary dimension  $v$ . The

required FLOPs for this operation is  $2BS^2hV$  in the forward pass and  $4BS^2hV$  in the backward pass, resulting in  $6BS^2hV$  FLOPs in total.

Thus, for a transformer model with  $l$  transformer layers, the total number of floating-point operations is:

$$96BS^2lh^2(1 + \frac{S}{6h} + \frac{V}{16lh}).$$